Mon. Not. R. Astron. Soc. **000**, 000–000 (0000) Printed 11 March 2013 (MN LATEX style file v2.2)

Constraints on the dark matter halo mass of Lyman-alpha emitting galaxies at z=3.1 from cosmic variance

Jaime E. Forero-Romero[1] and Julian Mejia[2]

[1]
[2]

11 March 2013

ABSTRACT

In this Letter we implement a new method to find the characteristic mass of dark matter halos hosting Lyman-Alpha Emitting (LAE) galaxies. The method is based on matching the statistics for the cosmic variance with the observations recently obtained by Yamada et al. (2012). We build a model for LAEs on top of a large N-body cosmological simulation (Bolshoi). The basic principle is that a dark matter halo can host one LAE with a probability $f_{\rm occ}$ if its mass is found withing a certain range mass range delimited by two threshold values, $M_{\rm min}$ and $M_{\rm max}$. We generate hundreds of mock catalogs in a thourough exploration of the parameter space of this model. These catalogs are constructed in such a way as to reproduce the spatial correlation between the different observed fields. We find that the models that best match the observed cosmic variance statistics are those with halo masses in the range $M_{\rm min}$ = and $M_{\rm max}$ = with and occupation fraction that scales as $f_{\rm occ}$ = with the minimum mass. We find that the angular correlation function is in agreement with the observational constraints.

Key words: galaxies: kinematics and dynamics, Local Group, methods:numerical

1 INTRODUCTION

Lyman-α emitting galaxies (LAEs) have become in the last decade a central topic in studies of structure formation in the Universe. The reason is the diverse range of fields where they are helpful, LAEs can be used as probes of reionization, tracers of large scale structure, signposts for low metallicity stellar populations and markers of the the galaxy formation process through cosmic history.

At the same time, theoretical and observational developments have contributed to the emergence of a paradigm to describe structure formation in a cosmological context. In this context it is considered that dominant matter content of the Universe is to be found in dark matter, whereby each galaxy is hosted by larger dark matter structure known as a halo.

Most models of galaxy formation find that the mass of the halo largely determines key properties of the galaxy such as its stellar mass and star formation rate. Processes that regulate the star formation cycle are also though to be strongly dependent on its mass. Furthermore, the spatial clustering of galaxies on large scales is entirely dictated by the halo distribution. For the reasons mentioned above, finding the typical dark matter halo mass hosting LAEs represents a significant step forward to understand the nature of this population in the context of LCDM.

Some theoretical approaches to this problem have been based on a forward modelling. Starting from the DM halo population, the corresponding intrinsic star formation properties are infered and statistics such as the luminosity function, the correlation function and the equivalent width distributions. Such modelling has been implemented from analytic considerations, semi-analytic models and full N-body hidrodynamical simulations.

Added to the uncertainties in the astrophysical processeses describing star formation in galactic populations, a highly debated steps in this approach is the calculation of the fraction of Lyman-α photons that escape the galaxy to the observer. Given the resonance nature of the line, the radiative transfer of Lyman-α is sensitive to the density, temperature, topology and kinematics of the neutral Hydrogen in the interstellar medium (ISM).

This complexity makes the use of monte-carlo simulations for the radiative transfer a required tool to obtain physically sound results, although the degeneracy in the physical parameters involved in the problem makes it difficult to achieve a robust consensus on what is the theoretical expected value for the Lyman-*alpha* escape fraction in high redshift.

Throughout this Letter we assume a ΛCDM cosmology with the following values for the cosmological parameters, $\Omega_m = 0.27$, $\Omega_\Lambda = 0.73$ and $h = 0.70$, corresponding to the matter density, vacuum density and the Hubble constant in units of 100 km s^{-1} Mpc^{-1}.

2 METHODOLOGY

In this Letter we constrain the typical mass of dark matter halos hosting LAES at $z = 3.1$. Our model is based on the number density information obtained in the recent large scale survey presented by XXX where XXX LAEs are detected over 7 fields of $\sim 46 \times 35 \mathrm{Mpc}^2 h^{-2}$ in area comoving in area corresponding to observed fields of XXX deg^2.

Both the spatial distribution and luminosities of the galaxies have, at least in a statistical sense, informatio to constrain theoretical model of LAEs. The most detailed theoretical models are also faced to diverse physical and astrophysical uncertainties in obtaining statistical prediction for the Lyman-alpha line. This uncertainties are largest impediment to consruct an ab-iitio model for LAEs.

In this Letter we want to step back and reduce the complexity of our model, with the sole objective of reproducing the cosmic variance in the number density of LAEs. Afterwards we will interpret the implications of this result for physical models for Lyman-alpha emitting galaxies.

Our model is based on the predictions of a large volume high resolution N-body simulation describing the gravitational dynamics of dark matter. We do not have an strong bias towards the theoretical expectation of what the mass of the dark matter halo hosting the galaxy should be. Instead, we fully explore the parameter space of our simplified model. The only cut we impose is that observed LAEs do not reside in dark matter halos with masses less than 10^{10}hMsun [citation].

In the following subsections we describe the most relevant features of the observational data, the N-body simulation we use, our model and its parameters together with the method to compare its predictions against observations.

2.1 The Observational Constraints

Our observational reference are the recently published results of a panoramic survey of LAES at z=3.1 by Yamada et al. (2012). This survey was conducted with the Subaru 8.2m telescope and the Subaru Prime Focus Camera, which has a field of view covering 34×27 arcmin, corresponding to a comoving scale of 46×35 Mpc h^{-1} at $z = 3.09$. The narrow band filter is centered at 4977 Åwith a 77Åwidth, corresponding to the redshift range $z = 3.062 - 3.125$ and 41 Mpc h^{-1} comoving scale for the detection of the Lyman-α line centered at $z = 3.09$.

The choice to have only one the data from Yamada et al 2012 as reference was made because their surveys is the largest in area with a set of homogenous conditions that define the LAE sample. Other surveys by XXX an XXX that cover similar regions, but they use different criteria on the equivalent width (EW) cuts to construct the LAE samples. Different cuts in the EW can change the number of LAEs to be included in the catalog. This cuts have an impact on the fainter LAEs which are more abundante than brighter ones. Different definitions of the EW cuts can yield number densities different by a factor of two [REF, I think Yamada has some numbers].

The survey covered four independent fields. The first is the SSA22 field of 1.38 deg^2 with 1394 detected LAEs, this field has been known to harbor a region with a large density excess of galaxies. The second observed region is composed by the fields Subaru/*XMM-Newton* Deep Survey (SXDS)-North, -Center and -South, with a total of 0.58 deg^2 and 386 LAEs. The third and fourth fields are the Subaru Deep Field (SDF) with 0.22 deg^2 and 196 LAEs, and the fild arotund the Great Observatory Optical Deep Survey North (GOODS-N) with 0.24 deg^2 and 185 LAEs. In Table 1 we summarize the values we use in throughout this paper for the each field, covered area, measured surface LAE number density and inferred number volume density.

2.2 The Simulation and Halo Catalogs

The Bolshoi simulation was performed in a cubic volume of 250 h^{-1} Mpc on a side. It includes dark matter distribution is sampled using 2048^3 particles, which translates into a particle mass of $m_\mathrm{p} = 1.35 \times 10^8\ h^{-1}\ \mathrm{M}_\odot$. The cosmological parameters are consistent with a WMAP5 and WMAP7 data with a matter density $\Omega_\mathrm{m} = 0.27$, cosmological constant $\Omega_\Lambda = 0.73$, dimensionless Hubble constant $h = 0.70$, slope of the power spectrum $n = 0.95$ and normalization of the power spectrum $\sigma_8 = 0.82$ [REF].

We use halo catalogs constructed with a Friend-of-Friends (FOF) algorithm with a linking lenght of 0.17 times the interparticle distance. We have veryfied that the main results we present in this paper also hold if instead we use halo catalogs constructed from a the Bound Density Maxima (BDM) algorithm (Klypin et al. 1999) that are defined to have an density of 200 times the critical density. The minimum halo mass in the models we construct in this Letter correspond to groups of ~ 75 particles. The catalogs were obtained from the publicly available Multidark database [1] (Riebe et al. 2011).

2.3 Populating Halos with LAEs

The model that populates halos with LAEs is based on a one-to-one correspondence: each halo can only host a single LAE. There are three physical parameters in the model: the halo mass range $M_\mathrm{min} < M_\mathrm{halo} < M_\mathrm{max}$ where LAEs reside and the fraction f_occ of such halos that effectively host a LAE. In what follows we will describe by the letter $\mathcal{M}$ a model defined by these three parameters M_min, M_max y f_occ.

We stress that we do not intent to build a model for the luminosity of each LAE. Physically speaking we are primarely interested in constraining the halo mass above which there are detectable LAEs. under the conditions defined by Yamada et al.

For each mode $\mathcal{M}$ we create mock field from disjoint volumes in the simulation with the same geometry probed by Suprime-CAM and the narrow band filter, namely $46 \times 35 \times 41\ h^{-3}\mathrm{Mpc}^3$ where the last dinemsion goes in the redshift direction, corresponding to a total area of 880 arcmin^2 for each mock field. There is a total $5 \times 7 \times 6 = 210$ of such sub-volumes in a snapshot of the Bolshoi simulation.

Next we group these 210 mock fields in three different ways to construct the LAEs number density distribution. The first way we follow the observational setup and constructs 15 different mock surveys, each one composed of 12

[1] `http://www.multidark.org/MultiDark/`

mock fields, out of which 7 correspond to contiguous sub-boxes in the simulation to mimick the whole SSA22, 3 are also contiguous between them but not to the first 7 fields to mimick the SXDS fields and finally 2 non-contiguous fields that correspond to the SDF and GOODS-North fields. This will produce 15 different distributions for the number density for a given model M. The second is similar to the first one. There aare 15 different mock surveys with 12 mock fields each, but this time each field corresponds to uncorrelated sub-boxes in the simulation. The third way in only has 1 mock survey containing all the 210 mock fields, in this setup there is only one predicted number density distribution for each model M

The advantage of these three sampling ways is that they allow us to explore the effects of both cosmic variance and the correlation between fields. Comparing the results of the first and second method will help us to quantify the effect of field correlation, while compating the first and the third method will serve us to gauge the impace of cosmic variance.

2.4 Model Sampling and Selection

We generate a series of models $\mathcal{M}$ with different input parameters$\{M_{\rm min}, M_{\rm max}, f_{\rm occ}\}$ as follows. $M_{\rm min}$ and $M_{\rm max}$ are allowed to take 30 different values evenly spaced by 0.1 dex, $M_{\rm min}$ ranges from $\log_{10} M_{\rm min} = 10.0$ up to $\log_{10} M_{\rm min} = 12.9$, while $M_{\rm max}$ range from $\log_{10} M_{\rm min} = 10.1$ up to $\log_{10} M_{\rm min} = 13.0$. The occupation fraction $f_{\rm occ}$ takes 100 different values from 0.01 to 1.00 regularly spaced by 0.01. In total the number of different sets of input parameters to be explored is $30 \times 30 \times 100 = 9 \times 10^4$.

For each model $\mathcal{M}$ we compute the LAE surface density distributions for the three different ways of grouping the mock fields, as described in the previous section. For each sub-volume we project the positions of the LAE hosting halos along the z direction and calculate its surface number density in units of sources per arcmin^2. For each number density distribution we perform a Kolmogorov-Smirnov againsg the 12 surface density observational values. From this test we obtain the value $0 < P < 1$ to reject the null hypothesis, namely that the two data sets come from the same distribution. In this paper we use values of $P > 0.1$ to consider that the simulated and observed number densities come from the same distribution.

3 RESULTS

3.1 Dark Matter Halo Number Density

We present first the results for the intergrated dark matter halo surface density as a function of halos mass for each one o the 210 sub-volumes in the Bolshoi simulation. This result allowsus to better understand the expected trends for the LAEs' preferred mass and the occupation fraction. Figure **??** show these results. The continous lines correspond to the subvolumes. The shadowed area indicates the surface density values for LAEs allowed by the observations.

From this Figure we can read which models cannot reproduce the observations. Regions in the plot where the halo surface density values are below the observational constraint correspond to high masses halo masses. For a LAE model

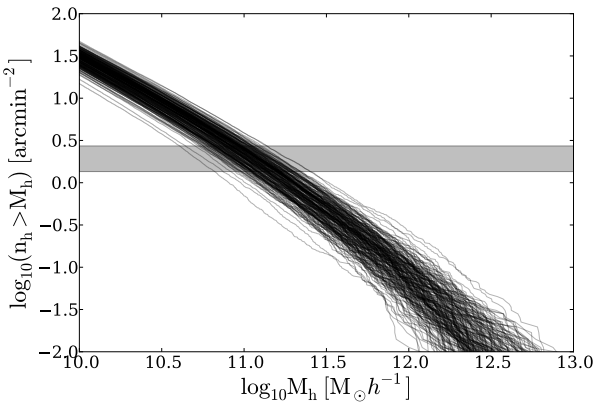

Figure 1. Cumulative mass function of dark matter haloes in the 210 sub-volumes of $46 \times 35 \times 41$ $h^{-3}Mpc^3$. The variation in the total number of dark matter halos per sub-volume evidences the effect of cosmic variance at such sub-volume scale. It is also appreciable the low population $\lesssim 10^{-3}h^2Mpc^{-2}$ of halos with $log(M/M_\odot) > 12.0$

.

Figure 2. $M_{\rm min}$-$M_{\rm max}$ plane for all models with $P > 0.1$.

$\mathcal{M}$ with a minimum mass $M_{\rm min}$ located in that mass range, the surface density is too low compared with observations.

Conversely, there are regions in the plot where the halo surface density can be higher than the observational constraints correspond to models $\mathcal{M}$ with a minimum mass below this threshold. Models with this minimum mass hava a chance for successfuly reproducing observations if the occupation fraction $f_{\rm occ} < 1$ is tuned as to lower the halo number density down to the observed value.

3.2 Selection of the preferred halo mass

Figure presents the regions in the parameter space $M_{\rm min} - M_{\rm max}$ where the KS test yields values of $P > 0.1$. Each panel corresponds to the three different ways of grouping the mock fields. In the case of the methods `Match` and `Random` the color code indicates the fraction of these 15 mock surveys with with $P > 0.1$. The third panel shows the result for the method `Full`, in this case the color code correspond to the value of P for a given model.

These results distinguish three mass regimes. In the first regime, at high mass values, we find that LAE models with minimum mass of $M_{\rm min} > XXX$ are not compatible with observations as expected from the analysis in the previous subsection. Below this mass down to $M_{\rm min} = XXX$ any minium and maximum mass models are compatible with LAEs observations. In a thirds mass regime, for low mass values $M_{\rm min} <$ only a limited range of models with $M_{\rm max}$ is able to reproduce observations.

In these three different mass regimes the occupation monotonically decreases as a function of the minimum halo mass $M_{\rm min}$. In Figure XXX we show this treend in three panels following the same correspondence as Figure XXX. From these results we interpret that the different mass

regimes that were identified correspond to best fit models with $f_{\rm occ} \sim 1$, $0 < f_{\rm occ} < 1$ and $f_{\rm occ} \sim 0$, respectively.

The two `match` and `random` methods present the highest number of matching mock surveys in the medium mass regime. However, it is important to keep in mind that not all the mock surveys for a sucessful model M present a high value $P > 0.1$, only a modest seems to be consistent with observations. This shows that the cosmic variance is still present on the physical scales probed by observations.

To illustrate this point, in Figure **??** we present the results for two mock fields for the `Match` method for a model with the same parameters, but two extreme values for the KS test.

Conversely there are different models where the KS test yield values of $P \sim 1$. To illustrate the kind of success represented by these models, we have selected these best ones in the case of the method `MatchObs`. Figure XXX shows in the main panel the spatial distribution of the mock surveys, the smaller panel shows the corresponding surface density distribution and the observational constraint.

3.3 Estimating the Galaxy Bias from the Halo Masses

Using the results from the previous sections it is possible to infre the bias of $z \sim 3$ LAEs. Considering a number of $N_{\rm fields}$ the expected number density of galaxies around the region located at x_i is $n_i = \bar{n}[1 + b\delta_{\rm DM}(x_i)]$, where $\bar{n}$ is the average galaxy number density and $\delta_{\rm DM} \equiv (\rho - \bar{\rho})/\bar{\rho}$ is the matter overdensity in the field [REF robertson].

We calculate the bias for each mock catalog in the best models using the corresponding dark matter overdensity in the simulation. This results in a distribution of bias values for each model. The results for this calculation are presented in Figure XX. We compare this resul agains the following estimation $b^2 \sim \sigma_N^2 - \bar{N}/\bar{N}^2\sigma_{\rm DM}^2$, where $\bar{N}$ is the average number counts in the N_{fields}, σ_N is their dispersion and σ_{DM} is the matter variance over many survey volumes.

3.4 Prediction for the angular correlation function

We calculate the angular correlation function (ACF) for the best models for a mock survey with a total surface area equal to the full survey by Yamada et al 2012. We compare these results with the observed ACF reported by Gawiser et al. XXX.

4 CONCLUSIONS

In this Letter we have constrained the preferred mass for dark matter halos hosting Lyman Alpha Emitters at a redshift $z = 3.1$. We use a method that matches the cosmic variance in the surface density number of LAEs from differente observed fields. From this we are able to constrain the mass range of dark matter halos hosting LAEs to be in the range $< M_{\rm h} <$ and a corresponding occupation fraction that escales as $f_{\rm occ} = M_{\rm min}$ with the minium halo mass defining the halo mass range.

In this letter, this estimate is based on a large Nbody simulation where we select a range a fraction of halos in a given mass range to host LAEs. We explicitly construct mock observations to derive statistics that can be compared against observations.

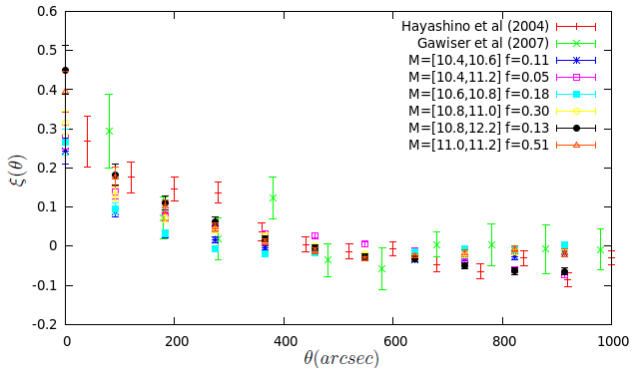

Figure 3.

The method is based on making an estimate of the cosmic variance from different observed fields. Based on a Nbody simulation, we select the range of halo masses, $M_{\rm min} < M_{\rm h} < M_{\rm max}$, and the fraction of these halos, $f_{\rm occ}$, that could host LAEs being compatible witht the cosmic variance constraints.

We have used a large volume cosmological N-body simulation that allows us to extract 210 sub-boxes each of which has a comparable volume to the field of view observed by Yamada et al. 2012. The comparison of the observed number density distribution against the results from our model is based on three different ways of constructing mock surveys. The first reproduces the spatial correlation between the 12 observational fields, the second breaks this spatial correlation while keeping the number of fields and the third one simply includes all the 210 sub-boxes.

ACKNOWLEDGMENTS

REFERENCES

Klypin A., Gottlöber S., Kravtsov A. V., Khokhlov A. M., 1999, ApJ, 516, 530

Riebe K., Partl A. M., Enke H., Forero-Romero J., Gottloeber S., Klypin A., Lemson G., Prada F., Primack J. R., Steinmetz M., Turchaninov V., 2011, ArXiv e-prints

Yamada T., Nakamura Y., Matsuda Y., Hayashino T., Yamauchi R., Morimoto N., Kousai K., Umemura M., 2012, AJ, 143, 79